

Supplementary material to:

**FINDING A CONSENSUS ON CREDIBLE FEATURES
AMONG SEVERAL PALEOCLIMATE RECONSTRUCTIONS**

BY PANU ERÄSTÖ*,†, LASSE HOLMSTRÖM†, ATTE KORHOLA‡ AND JAN
WECKSTRÖM‡,

National Institute for Health and Welfare, University of Oulu† and
University of Helsinki‡*

1. Reconstruction errors. In section 2 of the main paper the model for a reconstructed temperature anomaly \mathbf{y}_k is

$$(S.1) \quad \mathbf{y}_k = \boldsymbol{\mu}_k + \boldsymbol{\varepsilon}_k,$$

where $\boldsymbol{\mu}_k$ is the true temperature and $\boldsymbol{\varepsilon}_k$ is the reconstruction error. We report here some exploratory analyses of the properties of the errors $\boldsymbol{\varepsilon}_k$ as estimated by the residuals $\hat{\boldsymbol{\varepsilon}}_k = \mathbf{y}_k - \hat{\boldsymbol{\mu}}_k$, where $\hat{\boldsymbol{\mu}}_k$ is a smooth of \mathbf{y}_k . The smooths were computed using local linear regression with a Gaussian kernel where an optimal bandwidth selection method suggested in Ruppert, Sheather and Wand (1995) was employed.

The reconstructed temperature anomalies, their smooths and the associated residuals are depicted in Figure S.1. The bandwidths selected for reconstructions based on Lake Toskal diatoms and pollen were fairly large making the smooths almost linear. The sample standard deviations of the residuals are shown in Table S.1. They are somewhat smaller than the upper bounds $\bar{\sigma}_k$ in Table 2 of the main paper but still mostly larger than the alternative “small-error” value 0.2 used in the scale space analysis. A clear exception is the diatom based reconstruction for Lake Tsuolbmajavri for which the residual sample standard deviation is 0.13. Table S.1 indicates that the magnitudes of the reconstruction errors vary quite a bit for the six reconstructions and, on the basis of Figure S.1, at least the errors for the pollen based reconstructions may exhibit heteroskedasticity.

Q-Q plots of the residuals comparing the empirical quantiles of the residuals against standard normal distribution quantiles are displayed in Figure S.2. It appears that the distributions of the residuals could be considered at least roughly normal although a couple of values in the right tails

Proxy record	Std of residual
Lake Toskal chironomids	0.19
Lake Toskal diatoms	0.21
Lake Toskal pollen	0.54
Lake Tsuolbmajavri chironomids	0.3
Lake Tsuolbmajavri diatoms	0.13
Lake Tsuolbmajavri pollen	0.4

TABLE S.1

Sample standard deviations of the smoothing residuals for the 6 proxy records considered.

of the distributions for Lake Tsuolbmajavri chironomids and pollen appear suspiciously large. Histograms of the residuals are displayed in the diagonal plots of Figure S.4.

To explore error autocorrelation within each reconstruction we examined scatterplots of pairs of residual values. Thus, if the reconstruction errors in (S.1) are $\boldsymbol{\varepsilon}_k = [\varepsilon_{k1}, \dots, \varepsilon_{kj_k}]^T$, we plot the pairs $(\hat{\varepsilon}_{ki}, \hat{\varepsilon}_{k,i+1})$, $i = 1, \dots, j_k - 1$. This is referred to as “lag 1” scatter plot and similar plots were considered for lags 2 and 3. Some evidence for autocorrelation was found for Lake Toskal pollen and Lake Tsuolbma diatoms, both for lag 1 and 2 (cf. Figure S.3).

An attempt was also made to explore dependencies between different reconstructions. This was done by considering scatterplots of residual pairs $(\hat{\varepsilon}_{ki}, \hat{\varepsilon}_{lj})$, where k and l denote different reconstructions and i and j correspond to identical dates in their corresponding chronologies. Even after binning, the chronologies of some reconstructions overlap only partially and in these cases a rather small number of pairs could be plotted using this approach. For example, the overlap between the Lake Toskal Diatom chronology and the Lake Tsuolbma chronology is only 10 dates. The rationale for considering identical dates in the (binned) chronologies is that possible correlations between reconstructions would likely manifest themselves most strongly for such pairs of residuals. The results are shown in Figure S.4. None of the scatterplots were found to exhibit significant correlation, the smallest correlation coefficient p -value being 0.29 between Lake Toskal residuals for chironomids and pollen.

These preliminary analyses of the data suggest that the models considered in the main paper are quite reasonable. In particular, a multivariate normal error model for each reconstruction seems to be quite well justified. On the other hand, the more general model that allows prior correlation also between reconstructions may be unnecessarily complex.

2. Additional credibility maps. The feature maps of the main paper were based on the credibility level $\alpha = 0.8$. Figures S.5 and S.6 show maps

based on the credibility level $\alpha = 0.95$. As expected, fewer features are flagged as credible. Still, the main features exhibited by the lower credibility maps in Figures 8-10 of the main paper all still clearly visible.

Figures S.7 and S.8 show consensus analyses obtained with the model (6) of the main paper that allows dependencies both within the proxy records and between them. The result for large reconstruction errors (Figure S.7) looks quite similar to the corresponding map in the main paper (Figure 8). The result for small reconstruction errors (Figure S.8) has fewer features than the corresponding map for the simpler model (Figure 9 in the main paper). The exploratory analyses reported above suggested that our data may not require the more complex model and it might be that the more flexible error model interprets some of the actual features as correlated noise. Another explanation are potential convergence problems in the simulations. With the more complex model, computational issues quickly begin to limit the length of feasible MCMC runs. As in the main paper, Figures S.7 and S.8 here are based on samples of size 4000 where the first 2000 were used for burn-in. Instead of the 10 hours needed in the case of the simpler model, the more complex model required 4 days to generate a sample of this size.

References.

- Fox, J. and WEISBERG, S. (2011). *An R Companion to Applied Regression*, Second ed. Sage, Thousand Oaks CA.
- RUPPERT, D., SHEATHER, S. J. and WAND, M. P. (1995). An Effective Bandwidth Selector for Local Least Squares Regression. *Journal of the American Statistical Association* **90** 1257–1270.

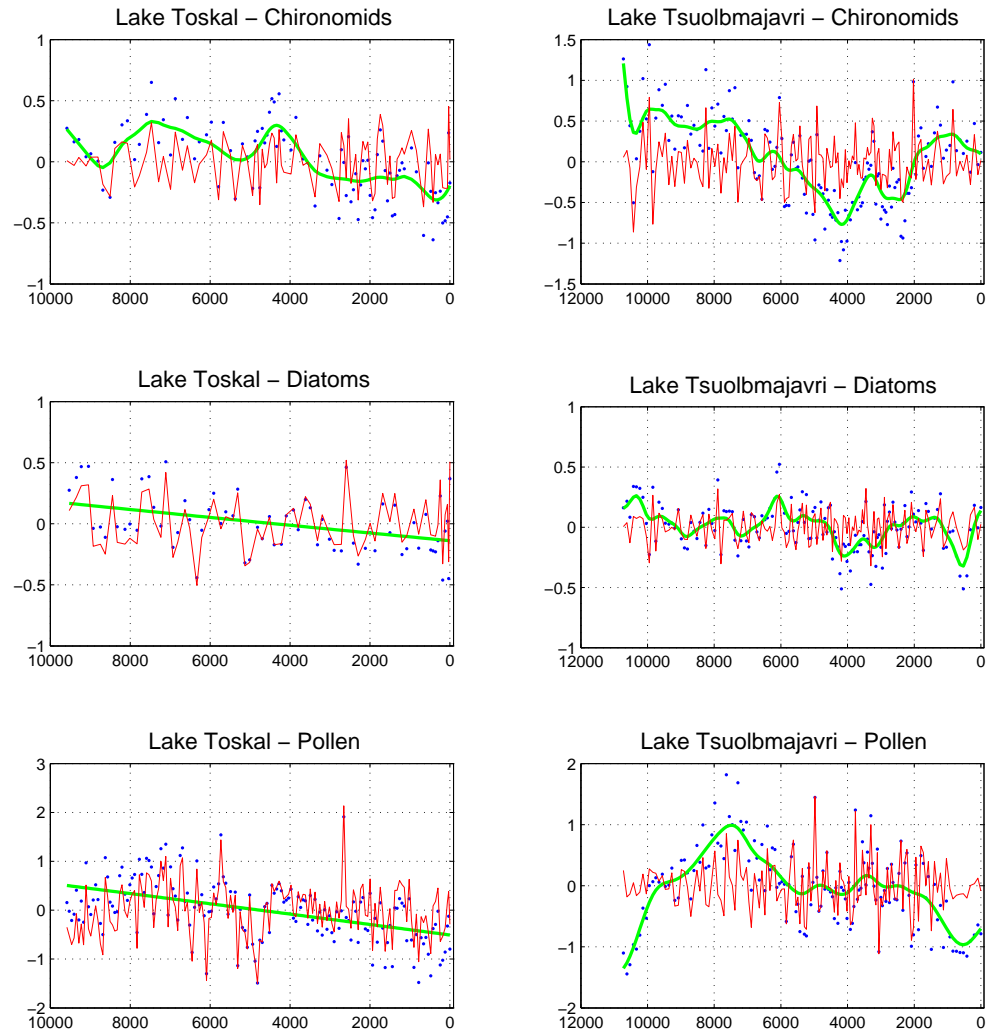


FIGURE S.1. Reconstructed temperature anomalies (blue dots), their smooths (green) and the smoothing residuals (red) computed as their difference. Smooths are local linear regressions with a Gaussian kernel where the bandwidths were computed using a method from Ruppert, Sheather and Wand (1995).

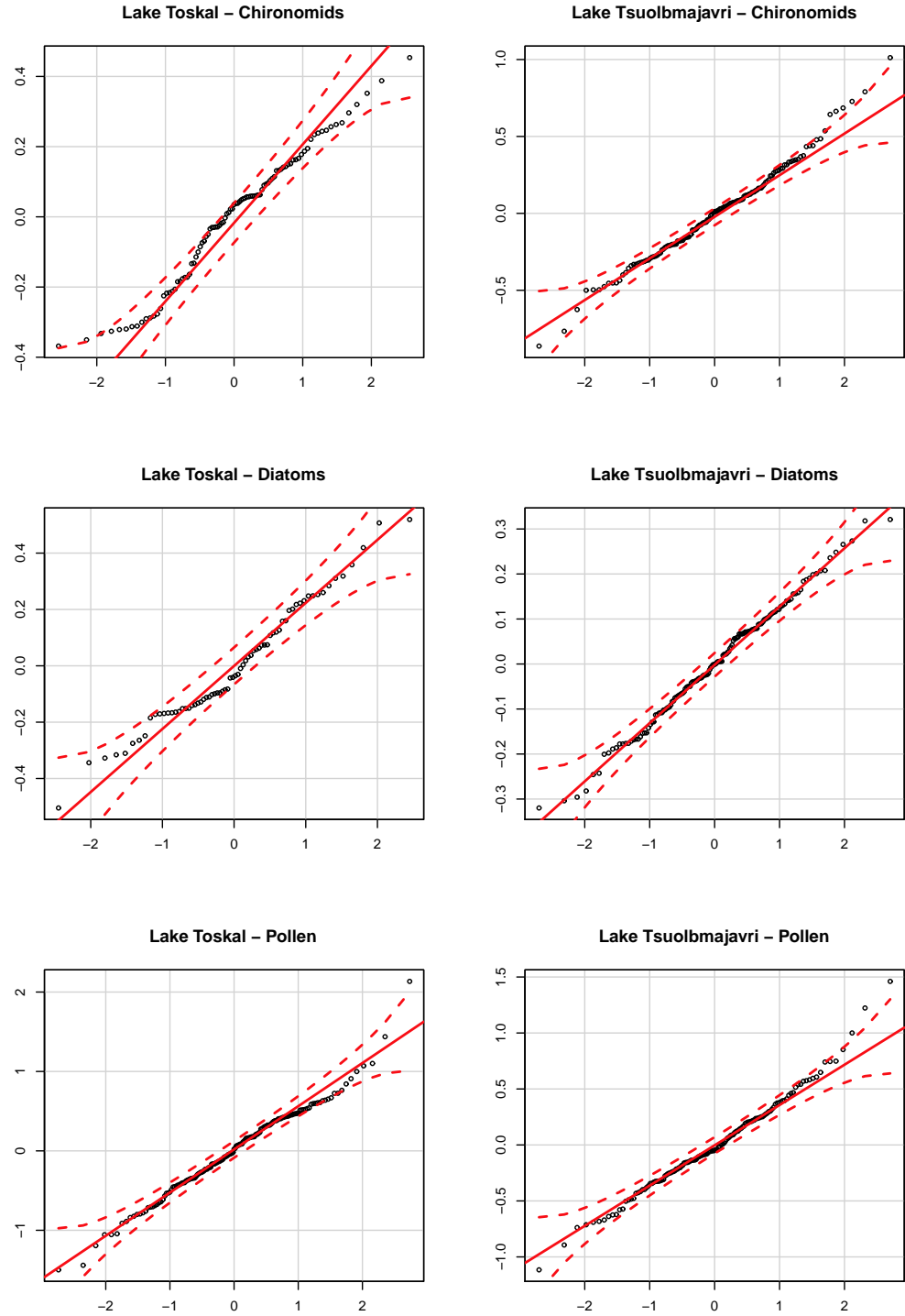


FIGURE S.2. *Q-Q plots that compare the empirical quantiles of the reconstruction errors estimated as smoothing residuals (vertical axes) against standard normal distribution quantiles (horizontal axes). The line passes through the first and the third quartiles and the dotted lines show the pointwise 95% confidence envelope. The plots were produced using the function qqPlot in the car R-package Fox and Weisberg (2011).*

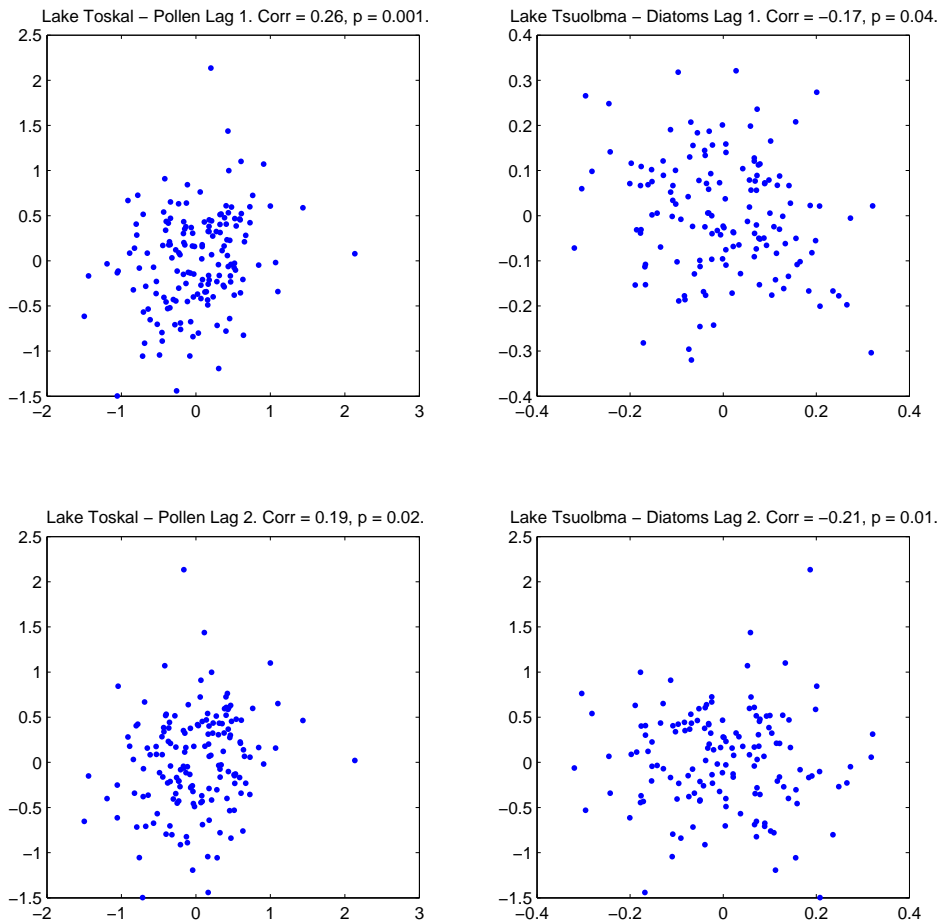


FIGURE S.3. Lag 1 and lag 2 scatter plots of reconstruction errors estimated as smoothing residuals for Lake Toskal pollen and Lake Tsuolbma diatom reconstructions. Also given are the estimated correlation coefficients and their p-values.

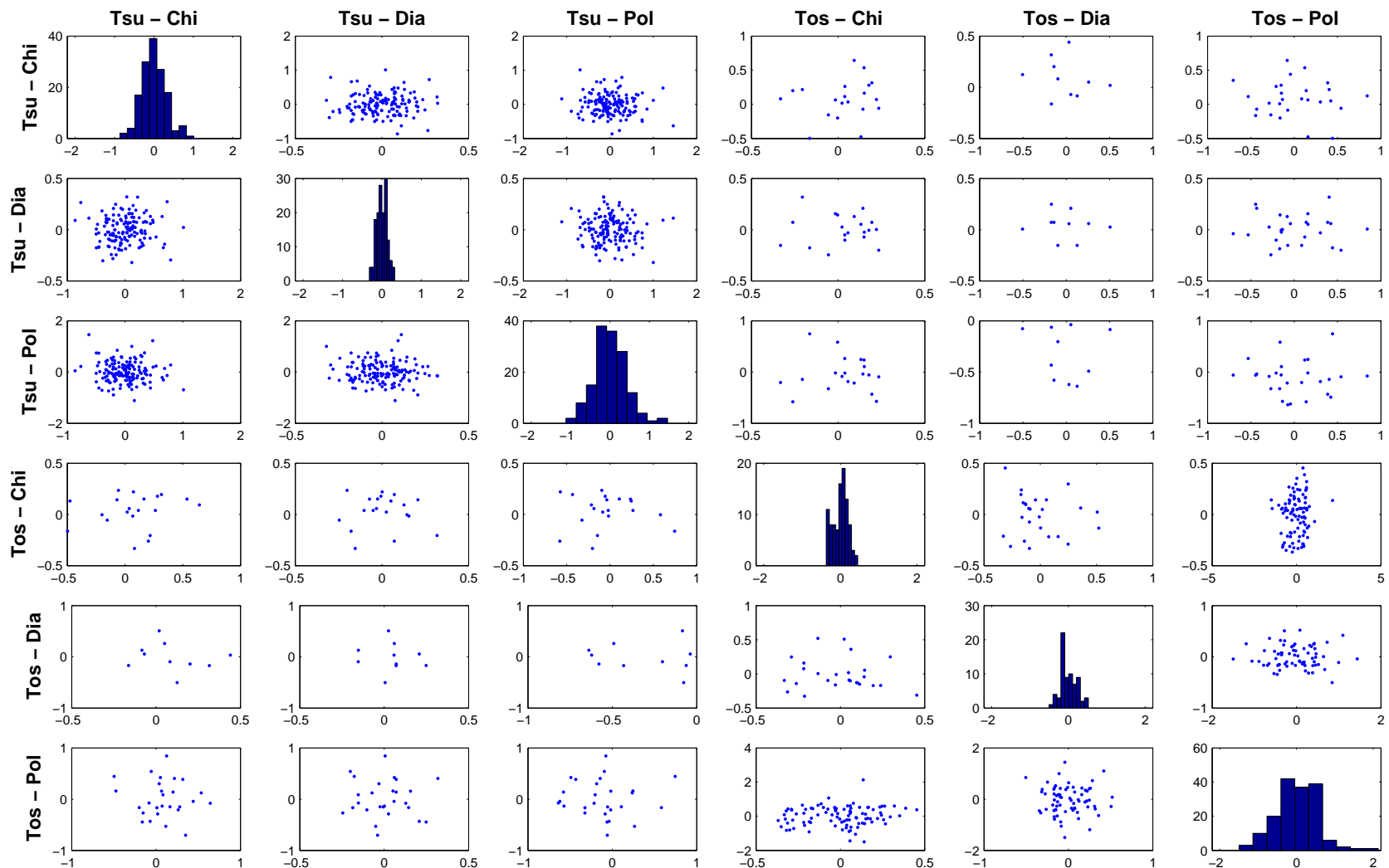


FIGURE S.4. Scatterplots and histograms of the reconstruction errors estimated as smoothing residuals. The dots mark pairs of residuals corresponding to the same dates in the two reconstructions considered. When the chronologies of two reconstructions differ, only errors corresponding to the dates common to the two chronologies are used in the scatter plots. Here "Tsu" and "Tos" stand for Lake Tsuolbmajavri and Lake Toskal, correspondingly, and "Chi", "Dia" and "Pol" stand for Chironomids, Diatoms, and Pollen, respectively.

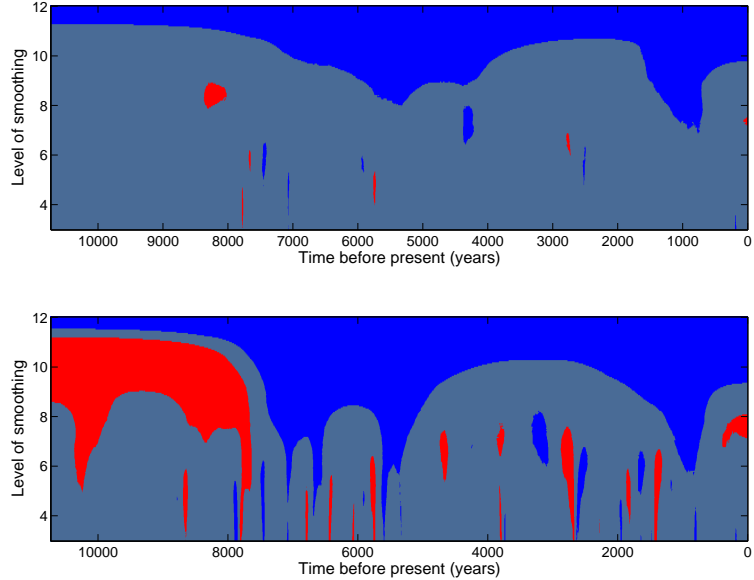


FIGURE S.5. Credibility maps for Holocene temperature consensus with posterior probability level $\alpha = 0.95$ when either large (upper panel) or small (lower panel) reconstruction errors are assumed. Blue and red indicate credible cooling and warming, respectively. For more information see the text in the main paper.

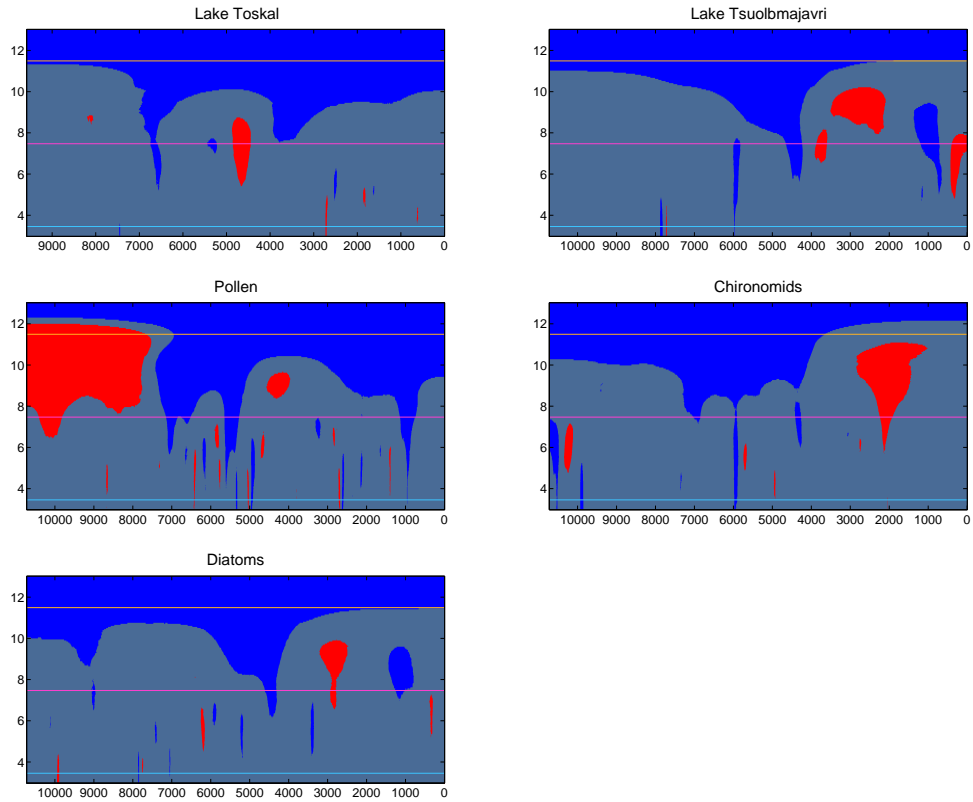


FIGURE S.6. Consensus based on subgroups of the six temperature reconstructions considered. Large reconstruction errors are assumed and the posterior probability level $\alpha = 0.95$. In the top row the two lakes are analyzed separately. The other three maps show the consensus according to each proxy. For more information see the text in the main paper.

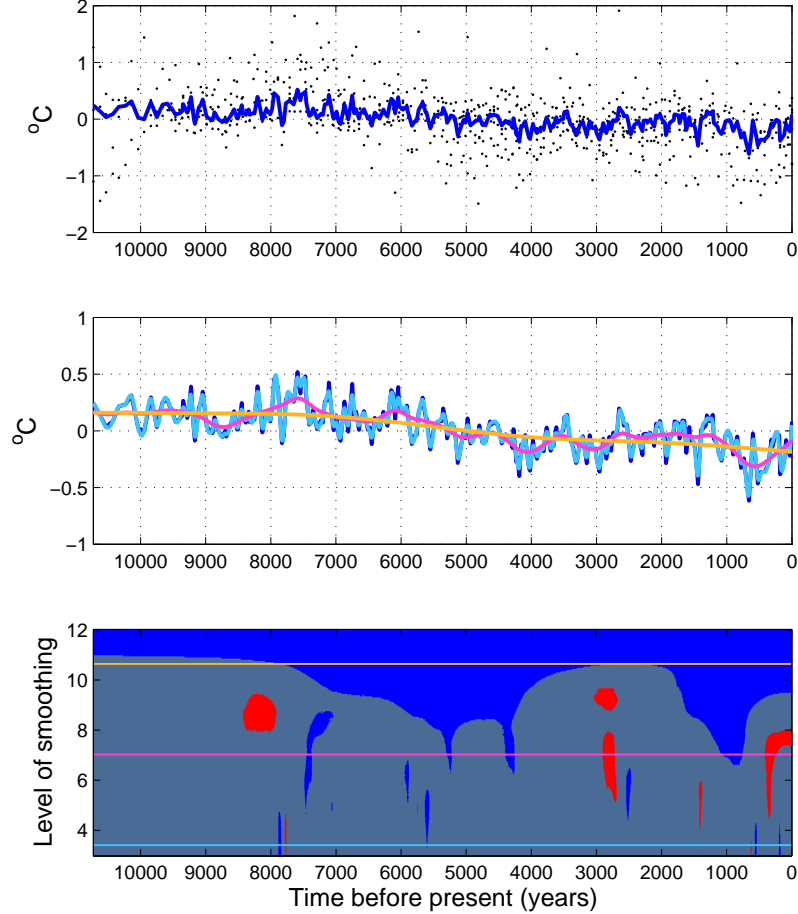


FIGURE S.7. *Scale space analysis of the consensus of six temperature reconstructions.* The model (6) in the main paper with large reconstruction errors is used and the level of credibility is $\alpha = 0.8$. The top panel shows the reconstructions (dots) and the posterior mean of the consensus (blue curve). The middle panel shows the posterior mean of the consensus together with three smooths of the posterior consensus corresponding roughly to multi-decadal (light blue), centennial (purple), and millennial (yellow) time scales. The bottom panel is the credibility map where blue and red indicate credible cooling and warming, respectively. For more information see the text in the main paper.

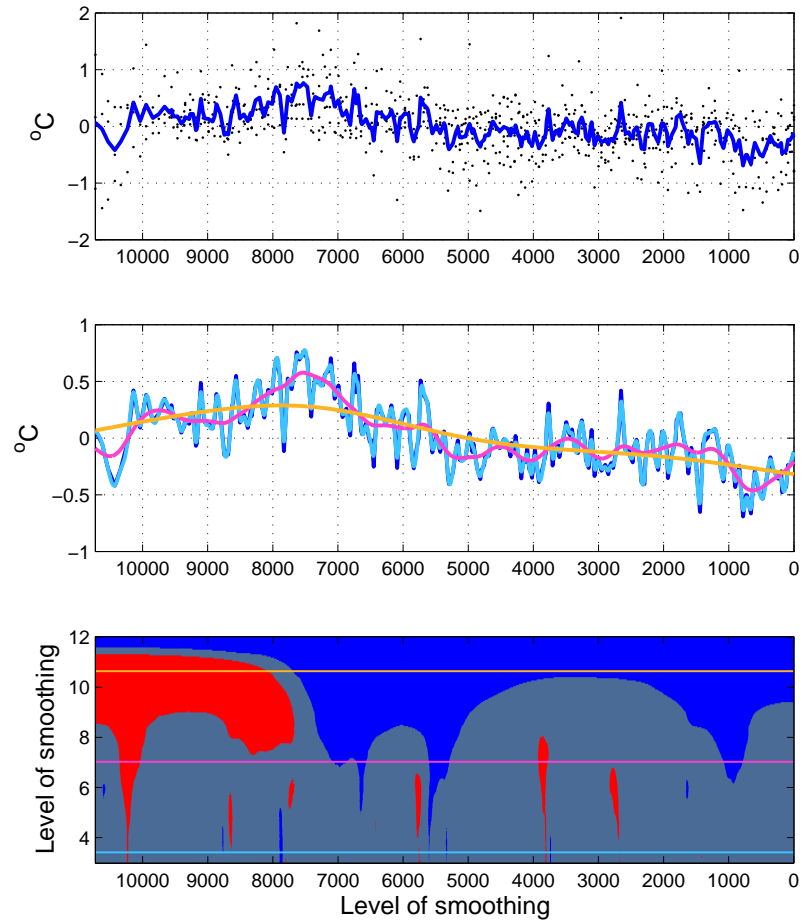


FIGURE S.8. Scale space analysis of the consensus of six temperature reconstructions. The model (6) in the main paper with small reconstruction errors is used and the level of credibility is $\alpha = 0.8$. For more information see the caption of Figure S.7 and the text in the main paper.

Table S.2. Sediment depths, calibrated ages, their standard errors and pollen-, chironomid- and diatom-based July mean temperature reconstructions for lakes Tsuolbmajavri and Toskal.

		Lake Tsuolbmajavri					Lake Toskal				
depth (cm)	age (cal BP)	error std	pollen	chironomids	diatoms	depth (cm)	age (cal BP)	error std	pollen	chironomids	diatoms
1	0	0	11.4	11.1	11.0	1	0	0	10.9	9.7	10.4
3	92	17	11.6	11.0	10.9	2	30	38	11.2	10.1	9.5
5	201	28	11.4	11.5	11.0	3	60	42	11.2	9.4	10.0
7	310	38	11.3	10.9	10.9	4	120	47	10.7	9.4	9.9
9	417	49	11.1	11.3	10.7	5	180	52	11.4	9.4	9.5
11	524	60	11.1	11.1	10.5	6	240	56	11.0	9.6	10.2
13	630	71	11.1	11.3	10.7	7	301	61	11.6	9.5	9.8
15	734	82	11.1	11.1	10.7	8	361	65	11.2	9.6	9.8
17	836	93	11.1	12.0	11.0	9	421	70	11.4	9.2	9.8
19	936	104	11.4	11.2	10.7	10	482	75	10.5	9.6	9.8
21	1034	114	12.0	11.1	10.8	11	542	79	10.6	9.9	
23	1129	121	11.2	11.0	10.8	12	602	84	10.9		10.1
25	1222	127	11.9	11.5	11.2	13	662	88	10.9	9.3	
27	1312	133	11.6	11.7	11.0	14	723	93	10.8		
29	1400	140	12.2	11.4	11.0	15	783	98	10.7		9.8
31	1486	146	11.2	11.0	11.0	16	843	102	11.0	9.8	
33	1569	153	12.4	11.2	11.2	17	904	107	10.9		10.0
35	1650	159	12.0	11.1	11.0	18	964	111	10.8	10.0	
37	1729	166	12.6	10.9	10.9	19	1024	116	11.8		
39	1805	172	12.7	11.4	11.0	20	1084	121	10.9		9.8
41	1879	177	11.5	11.3	11.0	21	1145	123	11.9	9.8	
43	1952	180	12.5	10.8	10.9	22	1205	123	11.5	9.9	9.7
45	2022	183	11.4	12.0	10.9	23	1265	122	11.4	9.8	
47	2090	185	11.2	10.7	11.2	24	1325	122	11.7	9.8	
49	2157	188	12.0	10.6	10.9	25	1386	122	11.4	9.4	10.1
51	2221	190	12.7	10.6	11.0	26	1446	121	10.6	9.4	
53	2285	193	12.6	10.3	11.2	27	1506	121	11.2	9.8	9.9
55	2346	195	11.8	10.1	11.0	28	1567	121	11.0	9.5	
57	2407	198	12.9	10.1	10.9	29	1627	121	11.1	9.8	
59	2466	200	12.4	10.8	11.0	30	1687	120	11.3	10.0	10.1
61	2523	202	12.0	10.8	10.9	31	1747	120	11.7	10.1	
63	2580	199	12.0	10.7	11.0	32	1808	120	11.2	9.9	
65	2636	196	12.3	10.9	11.1	33	1868	119	11.1	9.5	9.8
67	2690	194	12.6	10.4	10.9	34	1928	119	11.2	9.4	
69	2744	191	11.9	10.7	11.1	35	1989	119	11.9	9.6	9.9
71	2798	189	12.6	10.2	11.1	36	2049	119	11.5	9.9	
73	2850	186	11.9	10.3	10.7	37	2109	118	11.1	9.8	9.8
75	2902	183	12.0	10.4	11.0	38	2169	118	11.2	9.9	
77	2953	181	11.9	10.5	10.6	39	2230	118	11.7	9.7	
79	3004	178	12.0	10.3	10.7	40	2290	117	10.7	9.4	9.7
81	3055	178	11.1	10.9	10.7	41	2350	117	11.4	9.8	
83	3106	185	12.8	10.9	11.1	42	2411	117	11.8	9.6	9.8
85	3156	192	12.0	10.5	10.6	43	2471	119	11.9	9.5	
87	3206	198	12.2	11.3	10.8	44	2531	123	11.3	10.1	
89	3256	205	12.6	11.4	10.9	45	2591	128	11.4	9.6	10.4
91	3306	212	13.4	11.0	10.4	46	2652	132	13.2	9.9	
93	3356	219	12.5	10.9	10.7	47	2712	136	11.7	10.0	9.8
95	3406	225	12.8	11.0	10.8	48	2772	141	10.9	9.4	
97	3456	232	12.2	10.8	11.0	49	2833	145	11.7		
99	3506	239	12.6	10.8	10.8	50	2893	149	11.1		9.8
101	3556	245	12.9	10.5	10.9	51	2953	153	11.3	9.7	
103	3606	251	12.2	10.5	10.8	52	3013	158	11.5		9.9
105	3657	256	12.1	10.6	10.9	53	3074	162	11.3	9.8	
107	3708	262	12.0	10.4	10.7	54	3134	166	11.6		
109	3759	267	13.4	11.0	10.8	55	3194	171	11.0		10.0
111	3810	273	11.9	10.5	10.8	56	3255	175	11.6	9.9	
113	3862	278	11.6	10.5	10.7	57	3315	179	11.4		9.8
115	3914	284	11.5	10.3	10.6	58	3375	184	11.5	9.5	
117	3966	289	12.3	10.3	10.8	59	3435	188	11.7		
119	4019	295	11.7	10.0	10.7	60	3496	192	11.6		10.1
121	4072	299	12.0	10.4	10.9	61	3556	196	11.3	9.9	
123	4125	297	12.1	9.9	10.8	62	3616	198	11.7		10.2
125	4179	295	12.2	10.0	10.5	63	3677	200	11.5	9.9	
127	4233	294	12.4	9.8	10.6	64	3737	202	11.4		
129	4288	292	11.6	10.4	10.8	65	3797	204	11.9		9.9
131	4343	291	12.2	10.3	10.8	66	3857	206	11.5	10.2	
133	4398	289	11.7	10.7	10.8	67	3918	208	11.6		10.1
135	4454	287	12.0	10.3	10.7	68	3978	211	11.7	10.0	
137	4511	286	12.1	10.4	11.1	69	4038	213	11.9		

139	4568	284	12.1	10.5	11.0	70	4099	215	11.8		10.0
141	4625	285	12.7	10.7	10.8	71	4159	217	11.5	10.0	
143	4683	294	12.1	10.2	11.0	72	4219	219	11.5	10.1	9.8
145	4742	303	12.4	10.6	10.7	73	4279	221	12.0	10.4	
147	4801	311	11.9	10.7	11.2	74	4340	224	12.0	10.0	
149	4860	320	11.8	10.7	10.9	75	4400	226	12.1	10.4	9.8
151	4920	329	12.3	11.3	10.9	76	4460	228	11.9	10.4	
153	4981	337	13.6	10.0	11.0	77	4520	230	12.3	10.3	10.0
155	5043	346	12.3	10.4	11.0	78	4581	232	12.1	10.1	
157	5105	355	11.9	11.0	10.9	79	4641	234	11.1	10.0	
159	5167	364	12.5	11.0	10.8	80	4701	236	10.9	10.1	9.9
161	5230	370	11.4	10.4	11.2	81	4762	239	11.3	9.7	
163	5294	367	11.4	10.6	10.9	82	4822	241	10.1	10.1	10.0
165	5359	365	12.4	10.8	11.3	83	4882	243	9.8	10.0	
167	5424	363	11.5	11.3	11.1	84	4942	245	11.1	9.6	
169	5490	360	11.9	10.9	11.0	85	5003	247	11.0		9.7
171	5556	358	11.8	10.9	10.8	86	5063	249	10.5	9.9	
173	5623	356	12.9	11.2	10.9	87	5123	251	11.0		9.7
175	5691	353	12.7	11.0	11.1	88	5184	253	11.3	10.0	
177	5760	351	12.2	10.5	10.9	89	5244	254	11.3		
179	5829	349	11.6	10.5	10.9	90	5304	255	11.8		10.3
181	5899	347	12.2	10.5	11.0	91	5364	256	11.9	9.6	
183	5970	346	12.3	11.3	11.1	92	5425	257	11.6		10.0
185	6042	344	12.2	11.8	11.4	93	5485	258	11.4	10.0	
187	6114	343	12.2	11.2	11.5	94	5545	259	11.4		
189	6187	342	12.8	10.9	11.1	95	5606	260	12.0		10.1
191	6261	341	12.8	10.9	11.2	96	5666	261	12.3	10.2	
193	6335	339	12.5	11.2	11.1	97	5726	262	13.3		10.0
195	6411	338	13.2	11.4	10.9	98	5786	263	11.9	9.7	
197	6487	337	12.2	11.4	11.0	99	5847	264	11.9		
199	6564	336	12.9	10.5	11.1	100	5907	265	12.1		10.2
201	6641	336	12.3	10.8	10.8	101	5967	266	11.6	10.2	
203	6720	342	12.7	10.8	10.8	102	6028	267	11.5		10.1
205	6799	349	12.9	10.9	11.3	103	6088	268	11.4	10.1	
207	6879	355	12.1	11.3	11.1	104	6148	269	11.5		
209	6959	361	12.6	11.5	10.8	105	6208	270	11.7		9.9
211	7041	367	13.2	11.3	10.8	106	6269	271	12.1	10.0	
213	7123	373	13.1	11.3	11.0	107	6329	272	12.2		9.5
215	7206	379	13.3	11.3	10.9	108	6389	273	11.9	9.9	
217	7289	385	13.9	10.9	10.7	109	6450	274	11.6		
219	7373	391	12.8	11.9	10.8	110	6510	275	11.2		10.0
221	7458	398	13.2	11.5	11.0	111	6570	276	12.1	10.2	
223	7543	404	13.3	11.9	11.1	112	6630	277	11.7		10.2
225	7629	410	14.0	11.4	10.9	113	6691	278	12.5	10.0	
227	7716	416	12.6	11.6	11.0	114	6751	279	12.4		
229	7803	422	12.9	11.1	10.7	115	6811	281	11.6		9.9
231	7891	428	12.9	11.7	11.3	116	6872	282	11.9	10.4	
233	7980	435	13.6	11.4	10.9	117	6932	283	11.7		9.8
235	8069	442	13.0	11.7	11.2	118	6992	284	12.6	9.9	
237	8159	448	12.5	11.2	11.3	119	7052	285	11.5		
239	8249	455	12.5	12.1	10.9	120	7113	287	12.3		10.5
241	8339	461	13.2	11.1	10.9	121	7173	288	11.9	10.2	
243	8431	468	12.6	11.2	10.9	122	7233	289	13.1		10.0
245	8522	475	12.9	11.4	10.9	123	7294	290	12.3	10.0	
247	8614	481	12.5	11.5	10.9	124	7354	290	12.0		
249	8707	488	12.0	11.3	10.8	125	7414	290	11.4		10.1
251	8800	496	11.7	11.7	10.6	126	7474	291	12.3	10.5	
253	8893	508	12.6	11.2	10.8	127	7535	291	12.1		10.4
255	8987	521	12.6	11.6	10.6	128	7595	292	12.4	10.3	
257	9081	533	12.0	11.6	11.0	129	7655	292	11.9		
259	9176	546	12.0	11.2	10.8	130	7716	293	12.1		10.3
261	9270	558	12.5	11.6	10.9	131	7776	293	12.6	10.0	
263	9365	571	12.2	11.3	11.0	132	7836	293	12.3		9.9
265	9461	583	12.2	11.9	10.9	133	7896	294	12.1	9.9	
267	9557	596	12.4	11.7	11.0	134	7957	294	12.1		
269	9653	608	12.3	11.9	11.0	135	8017	295	12.1		10.0
271	9749	622	12.3	11.5	10.9	136	8077	295	11.9	10.2	
273	9845	638	12.3	10.9	11.2	137	8137	295	11.9		9.9
275	9942	654	12.2	12.4	10.7	138	8198	296	12.4	10.2	
277	10039	670	11.7	11.5	10.9	139	8258	296	12.2		
279	10136	686	11.8	12.0	11.1	140	8318	297	11.1		10.0
281	10233	702	11.4	11.4	11.0	141	8379	297	11.4	10.0	
283	10330	718	11.2	11.0	11.3	142	8439	297	11.4		10.3
285	10427	73									

287	10525	751	10.9	11.4	11.0	144	8559	298	11.9		
289	10622	767	10.8	11.9	11.0	145	8620	307	12.6		9.9
291	10719	779	11.1	12.3	11.0	146	8680	323	11.3	9.6	
						147	8740	339	10.9		10.0
						148	8801	355	11.3	9.9	
						149	8861	371	11.7		
						150	8921	388	11.3		9.9
						151	8981	404	11.4	9.9	
						152	9042	420	11.7		10.4
						153	9102	436	11.9	9.9	
						154	9162	452	11.4		
						155	9223	469	11.8		10.5
						156	9283	485	11.3	10.0	
						157	9343	501	11.9		10.4
						158	9403	517	11.6	10.0	
						159	9464	533	11.4		
						160	9524	550	11.3		10.3
						161	9584	558	11.4	10.1	